Relativistic analysis of Analyzing Power for $\vec{p}$ + ^{40}Ca & ^{208}Pb elastic scattering at 200 MeV

M. A. Suhail[1*] and N. Neelofer[2]

[1]Department of Physics, School of Physical Sciences, College of Natural and Mathematical Sciences,
The University of Dodoma, TANZANIA
[2]Physics Section, Women's College, Aligarh Muslim University, Aligarh-202002, INDIA
* email: m_asuhail@hotmail.com

Introduction

Developments over last few decades have given a good amount of reliability to the relativistic approach for the analysis of proton nucleus elastic scattering, particularly in the span of intermediate energies.

Here, we have adopted the relativistic Dirac phenomenological approach [1] to study the Analyzing Power (A_z) calculated for $\vec{p}$ + ^{40}Ca & ^{208}Pb elastic scattering at 200 MeV. In our analysis we have used three different nuclear ground state densities for both the targets. These densities are represented as LRAY, CHMX (as taken in ref. [2]) and NEG [3]. LRAY and CHMX are the experimental densities which incorporate medium corrections whereas NEG densities are purely theoretical microscopic densities for both the targets. To check the mass dependence we have calculated A_z for two different targets i. e. ^{40}Ca and ^{208}Pb.

In this approach the relativistic Dirac equation is reduced to the second order differential equation called as Schrödinger equivalent equation. This equation contains U_{eff} and U_{so} which represent the central and spin-orbit potentials respectively. These U_{eff} and U_{so} potentials are obtained in terms of scalar (U_s) and time-like component of the vector (U_0) potentials during reduction. The real parts of U_s and U_0 potentials are calculated from the folding model using nuclear ground state densities [1], whereas the imaginary parts have been taken directly from ref. [4]. Under folding model these potentials retain the shape of the densities used in their calculations. U_{eff} and U_{so} are very sensitive to the shape of U_s and U_0 potentials. If the densities used for the respective target are not realistic then U_s and U_0 will not yield accurate U_{eff} and U_{so} potentials and hence the data reproduction for scattering observables

will not be satisfactory. So, in our analysis we can easily pin-point which density is more reliable.

Further the comparison of A_z data calculated by fitting, using LRAY, CHMX and NEG densities for each target i.e. ^{40}Ca & ^{208}Pb manifests the importance of the medium corrections as well as the mass dependence.

The strengths of real and imaginary parts of complex U_s and U_0 potentials are multiplied with their respective normalization constants λ_s^r, λ_s^i, λ_v^r and λ_v^i. The complex U_s and U_0 potentials are then renormalized varying these λ's through chi-square minimization to fit the experimental data of elastic scattering observables. The values of λ's, if close to unity implies the accuracy of U_s and U_0 potentials and hence that of the nuclear matter densities involved.

Formalism

The Dirac equation is used in the mean field approximation in which the nucleon (meson) fields are replaced by their expectation values. Proton-nucleus scattering is then described using isoscalar-scalar and isoscalar-vector mean fields. Here, these are taken, respectively, as a spherically symmetric complex Lorentz scalar potential U_s corresponding to the σ meson field and a spherically symmetric complex Lorentz vector potential U_0 (time-like component of Lorentz four-vector), corresponding to the ω meson field, together with a spherically symmetric Coulomb potential V_c. With this scalar-vector interaction the Dirac equation becomes $(\hbar = c = 1)$

$$[\vec{\alpha} \cdot \vec{p} + \beta(m + U_s)]\psi = [E - U_0 - V_c]\psi, \quad (1)$$

where Ψ is a four-component Dirac spinor with upper (Ψ_U) and lower (Ψ_L) components, E is the

total energy of the scattered nucleon in the c.m. frame, $\bar{\alpha}$ and β are four Hermitian operators.

The second order reduction for the upper component Ψ_U yields,

$$\{p^2 + U_{eff} + U_{so}[(\vec{\sigma}.\vec{L}) - i(\vec{r}.\vec{p})]\}\psi_U =$$
$$[(E - V_c)^2 - m^2]\psi_U, \quad (2)$$

where U_{eff} is given by,

$$U_{eff} = \frac{1}{2E}[2EU_0 + 2mU_s - U_0^2 + U_s^2 - 2V_cU_0], \quad (3)$$

here $2V_cU_0$ is the Coloumb correction term. The corresponding spin-orbit term U_{so} is

$$U_{so} = -\frac{1}{2E}\left[\frac{1}{r}\left(\frac{1}{E + m + U_s - U_0 - V_c}\right) \times \frac{\partial}{\partial r}(U_s - U_0 - V_c)\right]. \quad (4)$$

Once U_s and U_0 potentials are known U_{eff} and U_{so} can be solved easily using eqs. 3 & 4. With these U_{eff} and U_{so} potentials, eq. 2 can be solved further for scattering observables.

Result and Discussion

Here we have allowed the strengths of the complex U_s and U_0 potentials to vary in chi-square fitting, but the geometries of these potentials are kept constrained.

As is clear from Fig.1(a), Analyzing Power at 200 MeV for $\vec{p} + {}^{40}$Ca is satisfactorily reproduced at forward angles by all the curves obtained using LRAY, CHMX and NEG densities. The curves corresponding to LRAY and CHMX densities are quite close to each other at all angles throughout the data though not reproducing the data well at higher angles. The curve obtained using NEG densities follow the data somewhat more closely even at higher angles although these (NEG) densities do not incorporate medium corrections. This shows that for $\vec{p} + {}^{40}$Ca elastic scattering at 200 MeV the geometry parameters of nuclear densities are more predominant compared to the medium corrections. Thus, one can conclude that NEG densities are better compared to the LRAY and CHMX densities particularly in this case.

When the Analyzing Power (A_z) is calculated for $\vec{p} + {}^{208}$Pb elastic scattering at 200 MeV it is found that the graphs obtained with LRAY and CHMX densities are close to the data compared to the graph obtained with the NEG densities at forward angles (Fig. 1 (b)). This may be attributed to the medium corrections which are incorporated in the LRAY and CHMX densities. All these graphs start deferring from data points as well as from each other at higher angles but still the graphs corresponding to LRAY and CHMX densities are comparatively closer to the data points at all angles. Again this shows the relevance of the medium corrections for heavier targets.
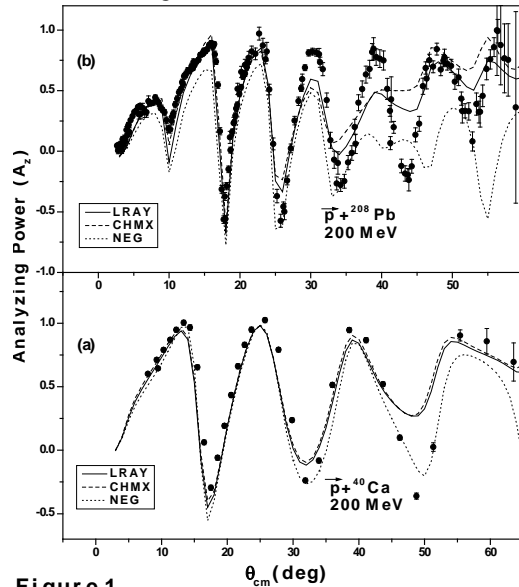

F i g u r e 1

At higher angles none of the graph is satisfactorily close to the experimental data of Analyzing Power for $\vec{p} + {}^{208}$Pb elastic scattering at 200 MeV. It simply implies that the geometry parameters of U_s and U_0, which are governed by the form of the densities employed, are playing a crucial role particularly in reproducing the data at higher angles. This effect is quite obvious in case of $\vec{p} + {}^{208}$Pb (Fig. 1(b)) rather than for $\vec{p} + {}^{40}$Ca elastic scattering (Fig. 1 (a)).

References

[1] L. G. Arnold, B. C. Clark, R. L. Mercer and P. Schwandt, Phys. Rev. **C23**, 1949 (1981).
[2] M. A. Suhail et al., Pramana-J of Phys., Vol. **65**, No. 6, 1027 (2005).
[3] J. W. Negele, Phys. Rev. **C1**, 1260 (1970).
[4] D. A. Hutcheon et al, Nucl. Phys. **A483**, 429 (1988).